

# Oblique impact: A process for providing meteorite samples of other planets.

*John D. O'Keefe and Thomas J. Ahrens*

Seismological Laboratory 252-21

California Institute of Technology

Pasadena, CA 91125

March 10, 1986

Cratering flow calculations for a series of oblique to normal ( $10^\circ$  to  $90^\circ$ ) impacts of silicate projectiles onto a silicate halfspace were carried out to determine whether the gas produced upon shock vaporizing both projectile and planetary material (which forms a downstream jet) could entrain and accelerate surface rocks and thus provide a mechanism for propelling SNC meteorites from the Martian surface. The difficult constraints that the impact origin hypothesis for SNC meteorites has to satisfy are that these meteorites are lightly to moderately shocked and yet were accelerated to speeds in excess of the Martian escape velocity ( $>5$  km/s). Two-dimensional finite difference calculations demonstrate that at highly probable impact velocities ( $\sim 7.5$  km/s), vapor plume jets are produced at oblique impact angles of  $25^\circ$  to  $60^\circ$  and have speeds as great as 20 km/s. These plumes flow nearly parallel to the planetary surface. It is shown that upon impact of projectiles having radii of 0.1 to 1 km, the resulting vapor jets have densities of 0.1 to  $1 \text{ g/cm}^3$ . These jets can entrain Martian surface rocks and accelerate them to velocities  $>5$  km/sec. We suggest that this mechanism launches SNC meteorites to earth.

N86-21479

Unclas  
G3/90 05682

(NASA-CR-176616) OBLIQUE IMPACT: A PROCESS  
FOR PROVIDING METEORITE SAMPLES OF OTHER  
PLANETS (California Inst. of Tech.) 16 p  
HC A02/MF A01 CSCI 03B



## Introduction and Background

All meteorites --- stones, irons, primitives, and differentiates --- are samples of other larger objects in the solar systems in that they exhibit features of planetary processes varying from: slight aqueous metamorphism (1), crystallization under different cooling histories (2), or crystallization in a substantial gravity field (3). The classes of stony meteorites, shergottites (S), nakhlites (N), and Chassigny (C), comprise only nine stones (4) collectively, called SNC meteorites which are unique in present terrestrial collections of  $\sim 10^4$  meteorites. The SNC meteorites are thought to be samples of Mars because:

(1) These have distinct crystallization ages of 1.3 Gy whereas all other meteorites (5) have a crystallization age of 4.6 Gy (6). Some discrepancies in ages are demonstrated by the more heavily shocked shergottites (4).

(2) The SNC meteorites show a distinctive  $\delta^{17}\text{O} - \delta^{18}\text{O}$  fractionation trend which is displaced from all other samples of the earth, the Moon, and other meteorites, including the petrologically similar basaltic achondrites (eucrites) (7).

(3) The shergottites are heavily shocked basalts with high volatile element abundances consistent with the Martian soil analyses (3). The lightly, or unshocked, nakhlites (clinopyroxenites) and Chassigny (dunite) appear to be more deep seated gravity cumulative rocks. Other evidence of formation on a planet with a strong gravity field comes from the general high degree of rare earth enrichment, the lack of an Eu anomaly, and the strong light rare earth element enriched pattern all suggesting the co-existence of garnet (9).

(4) Both the relative abundance and isotopic composition of the Ar, Kr, Xe, and N found trapped in the glass of the heavily shocked shergottites are uniquely different than noble gas ratios found in other meteorites, the earth or Venus (10). Their composition is close to that of the Martian atmosphere as measured by Viking. The gas provenance within the shock-induced glass in the shergottites implies that it was emplaced during an impact event on Mars in the Martian atmosphere. The  $^{40}\text{K}$ - $^{39}\text{Ar}$  reset time of 180 My in

the shergottites may record an impact event.

Cosmic ray exposure ages of 0.4-12 My (4) for SNC meteorites place important constraints on the size and/or transit time to the earth. If the impact age (180 My) corresponds to the time of ejection, then the low level of cosmic ray exposure can only be explained by the meteorite sample having been imbedded within an object having a diameter of  $\sim 10$  m. Conversely, if the 180 My event did not launch ejecta to velocities exceeding the Martian escape velocity, then 10 cm size objects are consistent with transit times on the order of the cosmic ray exposure age (11).

One of the key issues associated with the origin of SNC meteorites is how, if they are samples of a planet with substantial gravity, are they ejected from the planet and yet satisfy the above constraints? The entrainment of gases in the shock-induced glass, masklynite, within the shergottites with exactly the same number density per unit volume as in the Martian atmosphere as observed by the Viking landers (12) suggests that the samples were ejected from the planet by some aspect of the impact process. Several ejection mechanisms have been proposed. These include (1) normal impact ejection, (2) spallation, (3) impact vapor drag acceleration, and (4) shallow angle impact ejecta acceleration. None of the above mechanisms satisfies all of the constraints and/or is supported by detailed analysis and experiments.

(1) Ejection of material by near normal angle ( $> 80^\circ$ ) impacts is difficult because the planetary material is accelerated by a shock process. Simple shock state calculations as well as detailed impact flow field calculations show that silicate ejecta that has velocities exceeding the Martian escape velocity ( $> 5$  km/s) will be molten or partially vaporized (13). This conclusion is incompatible with the non- or lightly-shocked condition of the nakhlites and Chassigny, and only marginally agrees with the moderate shock history of the shergottites.

(2) Melosh (14) has proposed that the reflection of the impact shock wave from the planetary surface would result in spallation of the surface and ejection of lightly shocked

high speed fragments. His calculations imply that cm sized fragments could be ejected from the Moon but probably not from Mars. One of the major difficulties with this mechanism is that spallation fragments at high velocities have not been observed in impact experiments (15).

(3) Acceleration of impact ejecta and surface rocks by impact induced vapor has been proposed as a mechanism for producing high speed objects (16, 17, 18, 19). Singer (17) modeled a normal impact produced vapor plume as an expanding hemispherical cloud in which crater fragments were ejected and concluded that rocks greater than 1 m in diameter could not be accelerated to Martian escape velocities. Note that detailed numerical code calculations of normal, high-velocity impacts with substantial vaporization give vapor cloud plumes that are directed away from the surface and do not effectively entrain crater ejecta (13). Nyquist (18) proposed that a vapor cloud produced by a shallow angle impact ( $< 10^\circ$ ) would accelerate rocks to Martian escape velocities. The calculations presented here and experiments (20) show that significant vaporization does not occur in shallow angle impacts.

(4) Nyquist (18) suggested that multiple impacts of crater ejecta on surface rocks could accelerate them to Martian escape velocity without heavily shocking them. This mechanism is not consistent with the oblique impact calculations to be discussed below. Although Zook et al. (21) have shown enhanced ejecta production for impacts at oblique angles, this study did not demonstrate the combined constraints of high velocity but minimal shock metamorphism could be satisfied.

## **Approach**

We calculated the flow fields for normal and oblique impact using a two-dimensional numerical computational algorithm (22). The algorithm accurately models the flow field for normal impacts since in that case the flow has axial symmetry. In the case of oblique impacts, the two-dimensional model is an approximation to the three-

dimensional flow field and is only accurate in the plane described by the angle of impact. Thus we actually describe the oblique impact of a cylinder on a semi-infinite halfspace. The equation of state we employed was generic of silicates as they might exist on Mars. We assume a density and bulk modulus of  $2.7 \text{ g/cm}^3$  and 800 kbar. This would correspond to be 92% enstatite, mass fraction, and 8% water. The enthalpy of incipient vaporization is 3.3 kJ/g from STP or 0.85 of that of pure enstatite. The enthalpy of vaporization was taken to be  $\sim 12 \text{ KJ/g}$  and was varied from 0.12 KJ/g to 18 KJ/g to model effects of varying the volatility. The strength properties of the rock were neglected as those are unimportant in the modeling of high speed ejecta ( $> 1 \text{ km/s}$ ) (23).

Flow fields were calculated for impact angles ranging from 90 (normal impact), 80, 60, 45, 25, to  $10^\circ$ , and velocities characteristic of low speed (7.5 km/s) and high speed (20 km/s) events. The low speed is close to the mean value for impactors on Mars which is 8-12 km/s (24).

## Results

The resulting density and particle velocity flow fields for an impact velocity of 7.5 km/s are shown in figure 1. The vectors indicate the magnitude and direction of the velocity field and the contours delineate the density distribution. The nature of the flow field changes with impact angle and can be described in terms of three regimes: circular cratering, jetting, and skimming.

In the circular cratering regime nearly circular relatively deep craters are produced and the flow fields are initiated by a single shock process. This regime occurs for impact angles ranging from 90 to at least  $80^\circ$ . The fastest moving downstream ejecta velocity and angle of the ejection does not vary significantly with time. The ejecta are propelled at angles  $\sim 45^\circ$  relative to the planetary surface and this angle decreases to  $\sim 10^\circ$  as the impact angle decreased to  $\sim 45^\circ$ . For impact velocities of 7.5 km/s the initial high

speed ejecta is highly shocked and melted but not vaporized; for impact velocities of 20 km/s, the high speed ejecta is vaporized.

In the jetting regime, impact angle  $\sim 60$  to  $\sim 25^\circ$ , the crater is shallower and can exhibit complex configurations as has been shown in experiments (25). The ejecta velocity is approximately constant until jetting starts to occur at impact angles of approximately  $60^\circ$ . The maximum downstream ejecta velocity increases significantly with decreasing impact angle and reaches a maximum of nearly 20 km/s at oblique angles of  $\sim 25^\circ$  for impacts of 7.5 km/s (Fig. 2). The ejecta angle decreases rapidly with impact angle and much of the flow is within  $5^\circ$  of the surface for impact angles less than  $\sim 60^\circ$  (Fig. 2). The density contours show that the jet flowing across the surface is primarily low density vaporized planetary and impactor material. Qualitatively this flow is similar to those recently observed photographically by Schultz and Gault (20) upon oblique impact onto  $\text{CO}_2$ -bearing targets in the laboratory. The amount of mass vaporized is  $\sim 0.3$  the mass of the impactor for the 7.5 km/s and  $45^\circ$  case. The flow field in this regime is not solely initiated by a single shock process; multiple shock processes occur in the downstream direction and give rise to vaporization and jetting even at the relatively low impact velocity of 7.5 km/sec. The rapid increase in the downstream ejecta velocity to more than twice the impact velocity is a consequence of this jetting. The conditions for jetting are not satisfied for impact angles less than  $\sim 15^\circ$  (26). The downstream high speed ejecta consists of both planetary and impactor material for impact angles greater than  $\sim 25^\circ$  for low speed impactors.

The effect of varying the volatility of the planetary surface on the vapor plume was also examined. The vaporization energy was increased by a factor of 1.5 to simulate a refractory planetary surface (e.g., the moon) and decreased by an order of magnitude to simulate an extremely volatile-rich surface (e.g. Mars' polar regions). At an impact velocity of 7.5 km/s and angle of  $45^\circ$ , volatility did have a large effect on the jet plume characteristics. The plume velocity increased by 15% and the plume mass was within

10% of the nominal value for a decrease in vaporization energy of an order of magnitude. In the low vaporization energy case, the plume cloud was larger at a given time as compared to the nominal case, however, the density was lower. The reason for this is that the multiple shock region that creates the jet plume is localized, thus it restricts the amount of material that can be vaporized; in addition, the temperatures in that region are well above that required to vaporize even very refractory rocks. A greater difference would be expected at lower but less probable impact velocities, where the shock region is at the threshold for vaporization.

At impact angles less than  $\sim 25^\circ$ , the skimming regime occurs and the projectile is eroded as it skids along the planetary surface. No substantial penetration of the planetary surface occurs. In this case only the impactor material constitutes the small ejecta jet.

#### Entrainment of Surface Rocks

Examining the flow fields in figure 1 suggests that the the high velocity vapor plumes that are produced by oblique impacts could be a mechanism for accelerating surface rocks to velocities in excess of Martian escape velocity. We outline a simple model for determining the conditions for accelerating surface rocks under lightly shocked and unfractured conditions.

The present calculations are a good approximation to the flow field in the plane of incidence and close to the point of impact. We developed a model for the flow field in the plane of incidence which accounts for its out of plane expansion of the vapor. We found that the jet plume has a finite extension and flows along the planet surface.

The finite extent and duration of the cloud arises from the jet source, which is the multiple shock interaction region. The non-stationary vapor source propagates along the surface, and, being at the threshold for vaporization, provides vapor at a minimum expansion velocity.

For impact velocities of 7.5 km/s and impact angles ranging from 45 to 60°, the vapor plume was modeled as an expanding hemi-torus in the downstream direction. With this assumption, the vapor plume density as a function of distance along the surface is given by

$$\rho_g = \rho_{g0} \left( \frac{x_0}{x} \right) \left( \frac{r_0}{r(x)} \right)^2 \quad (1)$$

where  $\rho_{g0}$  is the mean computed density of the jet plume at a mean position  $x_0$  and  $r_0$  is the mean radius of the semi-circle (see figure 1d). The  $(x/x_0)$  term accounts for the decrease in density from expansion of the gas perpendicular to the plane of impact; the  $(r_0/r)$  term accounts for the radial expansion of the vapor plume in the plane of impact. Here  $r$  and  $x$  are the minor and major radii of the hemi-torus. The radius of the plume as a function of  $x$  is given by

$$r(x) = r_0 + v_r (x-x_0)/v_x \quad (2)$$

where  $v_x$  and  $v_r$  are the longitudinal and radial velocities of the plume.

We infer from experimental entrainments observed in chemical and nuclear explosive phenomena (27) that the high velocity jet plume will efficiently entrain rocks on a planetary surface.

The high velocity plume when impinging upon a surface rock fragment of density  $\rho_g$  will crush it unless the plume density is sufficiently low such that the stagnation pressure is less than the one dimensional, compressional strength,  $\sigma_c$ ; an upper bound is given by

$$\sigma_c = \rho_g v_x^2/2 \quad (3)$$

Given the density and size of the plume at the non-fracture position, an important issue is, what is the maximum size boulder which can be accelerated in excess of the Martian escape velocity (5.03 km/sec)? The maximum equivalent fragment radius,  $r_p$ , that can be accelerated to velocities on the order of the plume velocity is related to the



vapor plume radius at non-fracture position by

$$r_p = 3 \rho_g x / 2 \rho_p \quad (4)$$

where  $r_p$  and  $\rho_p$  is the fragment maximum radius and density. Equation 4 is derived from equating the mass of the fragment to the mass of gas required to accelerate it to escape velocity (28).

Equations 1-4 were solved to determine maximum radius fragment that could be accelerated by the jet plume as a function of impacting body radius without fracturing (Fig. 3). For impactors having radii in the range of  $10^{-1}$  to  $10^0$  km (which will result in craters with radii of  $10^0$  and  $10^1$  km), silicate surface fragments initially downstream of the ejecta jet having radii of at least 10 cm can be accelerated via gas entrainment to the Martian escape velocity.

The gas entrainment mechanism, even in the present two-dimensional approximation, is only slightly enhanced because of the likely higher level of  $\text{CO}_2$  and  $\text{H}_2\text{O}$  in readily volatilized forms in the the Martian regolith (29). Other selective mechanisms must operate to explain any preponderance of Mars samples brought to the earth in the form of SNC meteorites in preference to samples from the more refractory lunar surface (11).

Oblique impact induced jet plume entrainment appears to be the only mechanism which provides the physical mechanism required to explain the acceleration to high speed of lightly shocked planetary samples such as SNC meteorites.

## References

- 1: J. F. Kerridge and T. E. Bunch, in *Asteroids*, T. Gehrels, Ed. (U. of Ariz. Press, 1979), pp. 745-764.
- 2: J. T. Wasson, in *Meteorites*, (Springer-Verlag, 1974), 316 pp.
- 3: H. Y. McSween, Jr., *Geology*, **12**, 3 (1984).
- 4: H. Y. McSween, *Rev. Geophys.*, **23**, 391 (1985).
- 5: ALHA 81005 and Yamato 791193, which appear to be samples of the lunar highlands. A. Bischoff and D. Stöffler, [abs], *Lunar and Planetary Science XVI*, 63-64 (1985).
- 6: J. C. Laul, M. R. Smith, R. A. Schmitt, *Geophys. Res. Lett.*, **10**, 825 (1983).
- 7: T. K. Mayeda and R. N. Clayton, *Geophys. Res. Lett.*, **10**, 799 (1983).
- 8: ALHA77005, a shergottite, contains xenocrysts similar to assemblages in terrestrial basalts.
- 9: C. A. Wood and L. D. Ashwal, *Proc. Lunar Planet. Sci.*, **12B**, 1359-1375 (1981); H. Y. McSween and E. Jarosewich, *Geophys. Cosmochim. Acta*, **47**, 1501-1513 (1983); Garnet presence implies a pressure of  $\sim 12$  kbar and hence at least a Vesta-sized object.
- 10: R. H. Becker and R. O. Pepin, [abs.], *EOS (American Geophysical Union Transactions)*, **64**, 253 (1983); D. D. Bogard and P. Johnson, *Science*, **221**, 651 (1983).
- 11: G. W. Wetherill, *Meteorites*, **19**, 1-13 (1984).
- 12: V. Ott and F. Begemann, *Nature*, **317**, 509-512 (1985); R. O. Pepin, [abs.], *The Evolution of the Martian Atmosphere*, Lunar and Planetary Institute, (1985) pp. 20-21.
- 13: J. D. O'Keefe and T. J. Ahrens, *Proc. Lunar Sci. Conf. 8th*, 3357 (1977a); J. D. O'Keefe and T. J. Ahrens, *Science*, **198**, 1249 (1977b).
- 14: H. J. Melosh, *Icarus*, **59**, 234-260 (1984); H. J. Melosh, (abs.), *Lunar and Planetary Science XVI*, 548 (1985).

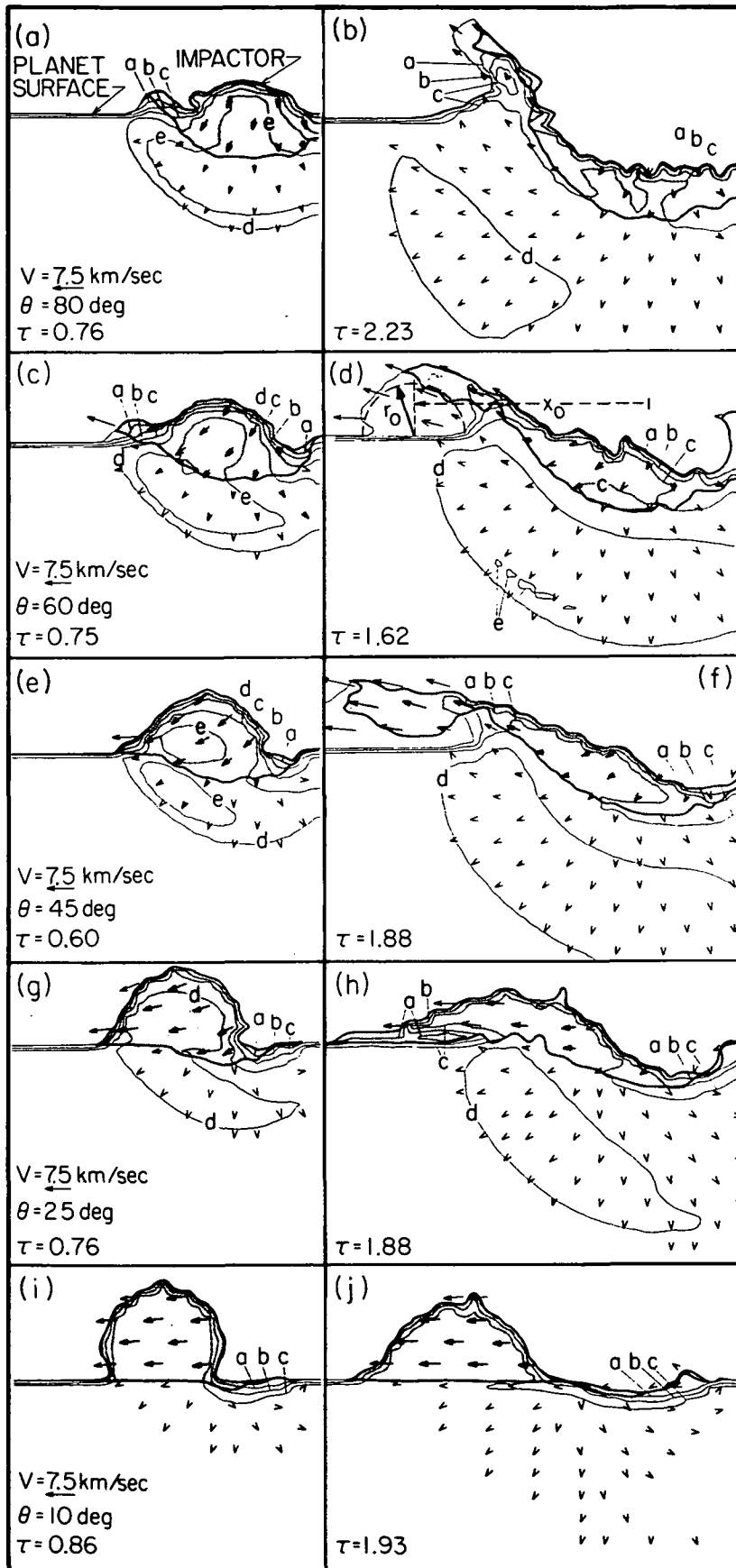
- 15: C. Polanskey and T. J. Ahrens, [abs.] *Lunar and Planetary Science XVI*, 671-672 (1985).
- 16: D. E. Rehfuss, *J. Geophys. Res.*, **32**, 6303 (1972).
- 17: A. V. Singer, [abs.] *Lunar and Planetary Science XIV*, 704-705 (1983).
- 18: L. E. Nyquist, *Proc. Lunar and Planet. Sci. Conf., 19th*, A785 (1982).
- 19: A. M. Vickery, [abs.], *Lunar and Planetary Science XVI*, 877-878 (1985).
- 20: P. N. Schultz and D. E. Gault, [abs.], *Lunar and Planetary Science XVI*, 740 (1985).
- 21: H. A. Zook et al., [abs.], *Lunar and Planetary Science XV*, 965 (1984).
- 22: S. L. Thompson, SAND 77-1339, Sandia National Labs, Albuquerque, N.M. (1979).
- 23: T. J. Ahrens and J. D. O'Keefe, *Impact and Explosion Cratering*, D. J. Roddy, R. O. Pepin, and R. B. Merrill, Eds. (Pergamon, New York, 1977) p. 639-656,
- 24: G. Neukum and D. V. Wise, *Science*, **194**, 1381 (1976).
- 25: D. E. Gault, *The Moon*, **6**, 32 (1973).
- 26: G. R. Cowan and A. H. Holtzmann, *J. Appl. Phys.*, **34**, 928 (1963); H. El-Sopky, in *Explosive Welding, Forming, and Compaction*, T. Z. Blazynski, Ed. (Applied Science Publishers, 1983), pp. 189-217. Kieffer, S. W., in *Impact and Explosion Cratering*, D. J. Roddy, R. O. Pepin, and R. B. Merrill, Eds. (Pergamon, New York, 1977, p. 251-770).
- 27: J. E. Schoutens, *Nuclear Geoplosics Sourcebook, Vol. IV - Part II*, Rep. DNA6501H-4-2, Defense Nuclear Agency, Washington, D. C., 1979. H. Minels, *Blowing model for turbulent boundary-layer dust ingestion*, SD-TR-85-97, The Aerospace Corp., El Segundo, CA (1986).
- 28: A. Henderson-Sellers, A. Benlow, and A. J. Meadows, *Q. J. R. Astron. Soc.*, **21**, 74-81 (1980).
- 29: J. T. Wasson and G. W. Wetherill, in *Asteroids*, T. Gehrels, Ed., (U. Ariz. Press, 1979), pp. 926-974.

30: Research supported under NASA Grant NSG 7129. We appreciate the assistance of Michael Lainhart with the calculations. We are grateful for the helpful comments on this MS proffered by A. Wetherill, D. Stevenson, D. Anderson, J. Melosh and M. Kovari. Contribution 4137, Division of Geological and Planetary Sciences, California Institute of Technology, Pasadena, California 91125.

Figure 1: Particle velocity and density flow fields for 2.6 g/cm<sup>3</sup> silicate projectile impacting silicate planet at 7.5 km/sec at oblique angles of 80° (a,b); 60° (c,d), 45° (e,f), 25° (g,h); and 10° (i,j). Density contours a=1.5, b=2.0, c=2.5, d=3.0 and e=3.5 g/cm<sup>3</sup>. Non-dimensional time,  $\tau$ , is real time times impact velocity divided by projectile diameter.

Figure 2: Downstream ejecta velocity versus impact angle for 7.5 and 20 km/sec silicate projectile impacting silicate planet (left). Range of angles between downstream ejecta plume flow direction and planetary surface for 7.5 km/sec impact (right). Bars represent range of values observed in calculated flow fields.

Figure 3: Surface fragment radius accelerated to 5 km/sec by gas flow in ejecta plume, versus impactor radius. Lines shown for surface fragments which will survive acceleration via  $\sigma_c = 1$  and 0.1 kbar stagnation pressure in flows with initial densities ( $\rho_{g0}$ ) of 0.1 and 1 g/cm<sup>3</sup> for vaporized planetary and projectile material. Values of  $v_x = 12$  km/sec,  $v_r = 3.3$  km/sec and  $x_0/r_0 = 5.0$  for 7.5 km/sec impact, are assumed.



TJA85113SP

Fig. 1

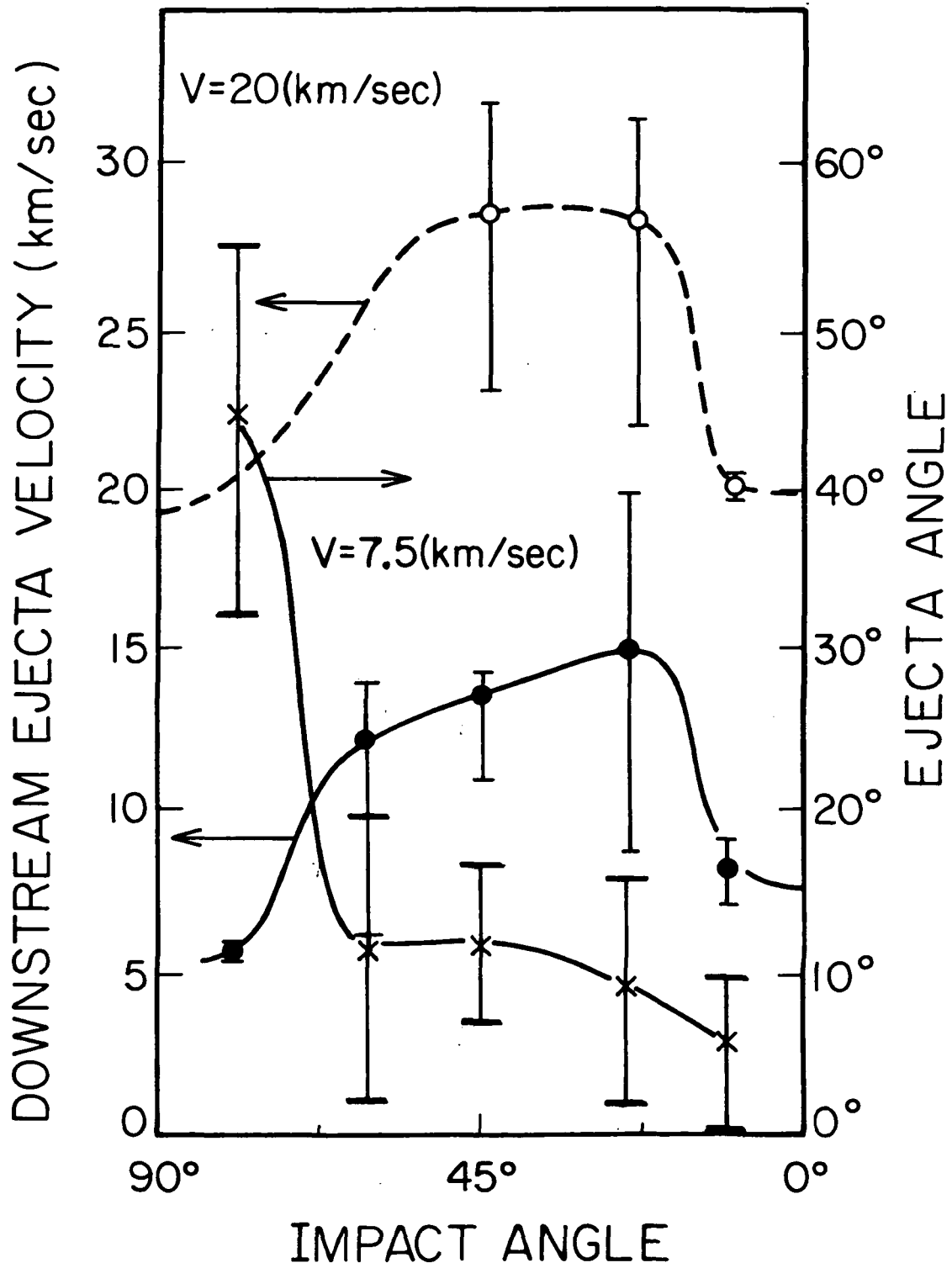


Fig. 2

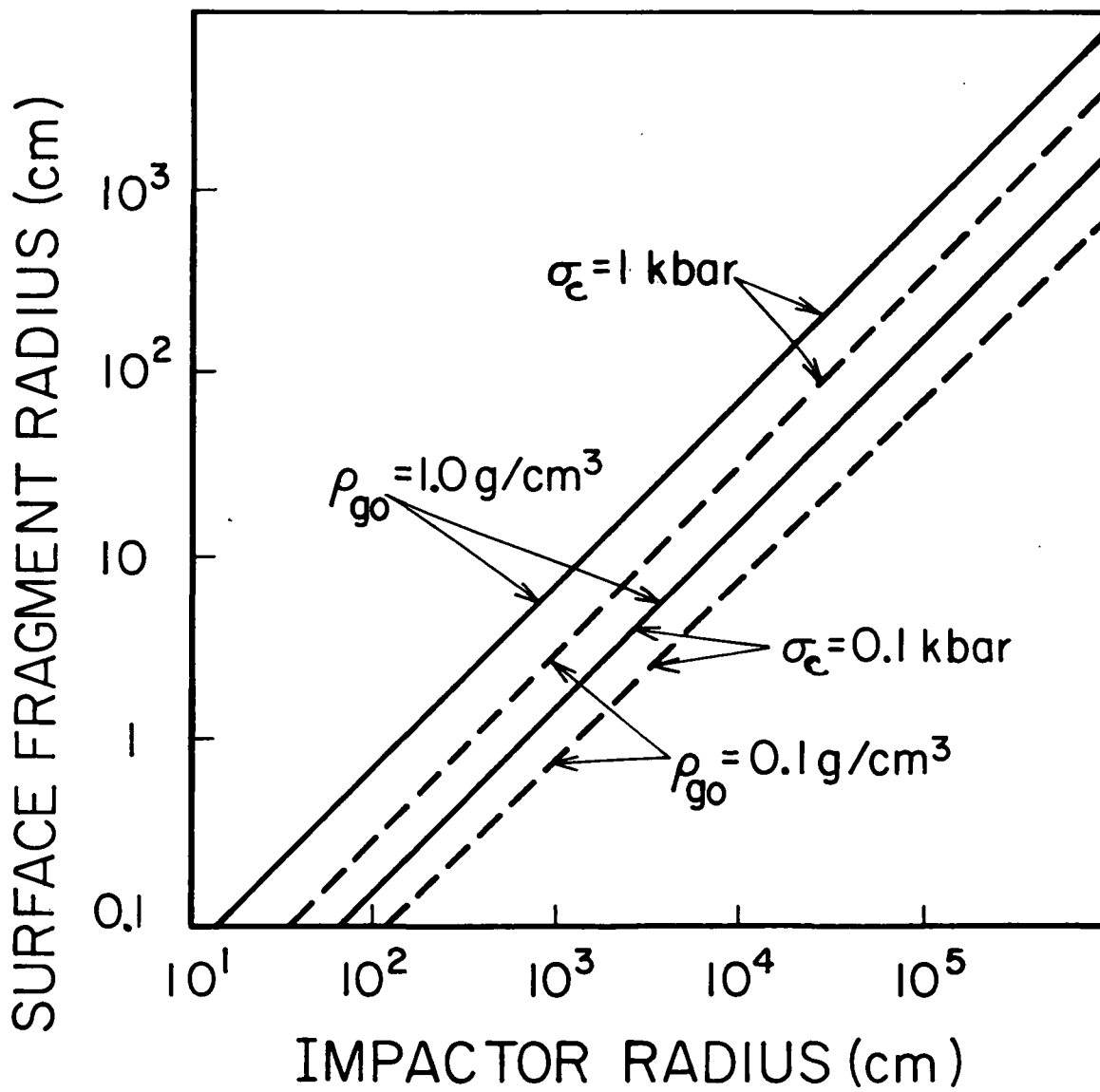


Fig. 3

TJA86018SFD